

The impact of soil microorganisms on the global budget of $\delta^{18}\text{O}$ in atmospheric CO_2

Lisa Wingate^{a,b,1,2}, Jérôme Ogée^{b,1,2}, Matthias Cuntz^{c,1,3}, Bernard Genty^{d,e}, Ilja Reiter^{d,e}, Ulli Seibt^f, Dan Yakir^g, Kadmiel Maseyk^{f,g}, Elise G. Pendall^h, Margaret M. Barbourⁱ, Behzad Mortazavi^{j,k}, Régis Burlett^b, Philippe Peylin^f, John Miller^{l,m}, Maurizio Mencuccini^a, Jee H. Shimⁿ, John Huntⁱ, and John Grace^a

^aSchool of GeoSciences, University of Edinburgh, Edinburgh EH9 3JN, United Kingdom; ^bUnité de Recherche 1263 Ecologie Fonctionnelle et Physique de l'Environnement, Institut National de la Recherche Agronomique, 33130 Villenave d'Ornon, France; ^cMax Planck Institute for Biogeochemistry, 07701 Jena, Germany; ^dLaboratoire d'Ecophysiologie Moléculaire des Plantes, Institut de Biologie Environnementale et de Biotechnologie, Service de Biologie Végétale et de Microbiologie Environnementale, Commissariat à l'Energie Atomique, 13108 Saint-Paul-lez-Durance, France; ^eUnité Mixte de Recherche Biologie Végétale et Microbiologie Environnementales, Centre National de la Recherche Scientifique, 13108 Saint-Paul-lez-Durance, France; ^fUnité Mixte de Recherche 7618 Biogéochimie et Ecologie des Milieux Continentaux, Centre National de la Recherche Scientifique/Université Pierre et Marie Curie, 78850 Thiverval-Grignon, France; ^gDepartment of Environmental Sciences and Energy Research, Weizmann Institute of Science, Rehovot, 76100, Israel; ^hDepartment of Botany, University of Wyoming, Laramie, WY 82071; ⁱLandcare Research, P.O. Box 40, Lincoln 7640, New Zealand; ^jDepartment of Biological Sciences, University of Alabama, Tuscaloosa, AL 35487; ^kDauphin Island Sea Lab, Dauphin Island, AL 36528; ^lNational Oceanic and Atmospheric Administration Earth System Research Laboratory, 325 Broadway R/GMD1, Boulder, CO 80305; ^mCooperative Institute for Research in Environmental Sciences, University of Colorado, Boulder, CO 80309; and ⁿDepartment of Forest, Rangeland, and Watershed Stewardship, Colorado State University, Fort Collins, CO 80523

Edited by Christopher B. Field, Carnegie Institution of Washington, Stanford, CA, and approved October 22, 2009 (received for review May 13, 2009)

Improved global estimates of terrestrial photosynthesis and respiration are critical for predicting the rate of change in atmospheric CO_2 . The oxygen isotopic composition of atmospheric CO_2 can be used to estimate these fluxes because oxygen isotopic exchange between CO_2 and water creates distinct isotopic flux signatures. The enzyme carbonic anhydrase (CA) is known to accelerate this exchange in leaves, but the possibility of CA activity in soils is commonly neglected. Here, we report widespread accelerated soil CO_2 hydration. Exchange was 10–300 times faster than the uncatalyzed rate, consistent with typical population sizes for CA-containing soil microorganisms. Including accelerated soil hydration in global model simulations modifies contributions from soil and foliage to the global CO^{18}O budget and eliminates persistent discrepancies existing between model and atmospheric observations. This enhanced soil hydration also increases the differences between the isotopic signatures of photosynthesis and respiration, particularly in the tropics, increasing the precision of CO_2 gross fluxes obtained by using the $\delta^{18}\text{O}$ of atmospheric CO_2 by 50%.

carbon cycle | water cycle | carbonic anhydrase | oxygen isotopes | terrestrial biosphere

The Earth's climate system is intimately connected to the movement of water and carbon across the planetary surface. As global warming proceeds, it is expected that photosynthetic CO_2 uptake will increase in colder regions of the world and diminish in those regions that are already warm and dry (1). At the same time, warming is expected to increase microbial activity, at least where water is not limiting, and therefore lead to an enhanced breakdown of organic matter in the soil, producing a large respiratory flux of CO_2 back to the atmosphere (2). Because terrestrial ecosystems presently sequester about a quarter of the CO_2 emissions associated with fossil fuel burning (7.1 GtC y^{-1}) (1), it is critical that we understand how large-scale, climate-driven changes will affect the carbon sequestration of the terrestrial biosphere. Currently, the precise response of terrestrial CO_2 sources and sinks to changes in climate remains uncertain (3) and its understanding requires the ability to quantify the amount of CO_2 taken up during photosynthesis separately from the amount released by respiration.

The oxygen isotope composition of atmospheric CO_2 (δ_a) was shown to be a powerful tracer of photosynthetic and respiratory CO_2 fluxes while at the same time providing information on the intensity of water cycling within terrestrial ecosystems (4–6). This tracing property occurs because the oxygen isotope composition ($\delta^{18}\text{O}$) of leaf and soil water pools is transferred to

atmospheric CO_2 during photosynthetic and respiratory CO_2 exchange, via an isotopic exchange during CO_2 hydration (7): $\text{CO}_{2\text{aq}} + \text{H}_2^{18}\text{O} \rightleftharpoons \text{CO}^{18}\text{O}_{\text{aq}} + \text{H}_2\text{O}$. Despite the short residence time of CO_2 in leaves, CO_2 involved in photosynthesis is nearly completely relabeled by ^{18}O -enriched leaf water because of the enzyme carbonic anhydrase (CA; EC 4.2.1.1), a very efficient catalyst of CO_2 hydration and isotopic exchange (4, 5, 8, 9). Typically the $\delta^{18}\text{O}$ of leaf and soil water pools are very different. There is a tendency for the heavier molecules of water to accumulate more readily in leaves than in soils during evapotranspiration because of the difference in water pool size (10, 11). Because the CO_2 - H_2O exchange in leaves (associated with photosynthesis) or soils (associated with soil respiration) produces such contrasting ^{18}O signals, estimates of the amount of CO_2 exchanged during photosynthesis and respiration can in principle be constrained by using the $\delta^{18}\text{O}$ signal of atmospheric CO_2 (6, 12).

However, our ability to partition gross fluxes of CO_2 may be complicated because the $\delta^{18}\text{O}$ of soil water (δ_{sw}) can often display a strong vertical gradient at the soil surface because soil evaporation also leads to an enrichment of heavy water molecules in the uppermost layers (13–15). Thus, to determine the $\delta^{18}\text{O}$ of CO_2 exchanged between soils and the atmosphere accurately it becomes necessary to know the shallowest depth (z_{eq}) where diffusing CO_2 molecules (from the atmosphere or produced by soil respiration; Fig. 1A) have enough time to fully equilibrate isotopically with soil water. With increasing temperature and moisture, CO_2 hydration increases relative to the diffusion rate so that z_{eq} moves closer to the surface, and toward more enriched $\delta^{18}\text{O}$ values (see *Methods*, Eq. 4). Although we know that CA accelerates the rate of hydration in leaves, the possibility of CA activity in soils is commonly neglected (4, 15),

Author contributions: L.W. and J.O. designed research; L.W., J.O., M.C., B.G., I.R., D.Y., K.M., E.G.P., M.M.B., B.M., R.B., J.M., M.M., J.H.S., J.H., and J.G. performed research; P.P. contributed analytic tools; L.W., J.O., M.C., B.G., I.R., and U.S. analyzed data; and L.W., J.O., U.S., and D.Y. wrote the paper.

The authors declare no conflict of interest.

This article is a PNAS Direct Submission.

¹L.W., J.O., and M.C. contributed equally to this work.

²To whom correspondence may be addressed. E-mail: l.wingate@ed.ac.uk or jogee@bordeaux.inra.fr.

³Present address: Helmholtz Centre for Environmental Research, Zentrum für Umweltforschung, 04318 Leipzig, Germany.

This article contains supporting information online at www.pnas.org/cgi/content/full/0905210106/DCSupplemental.

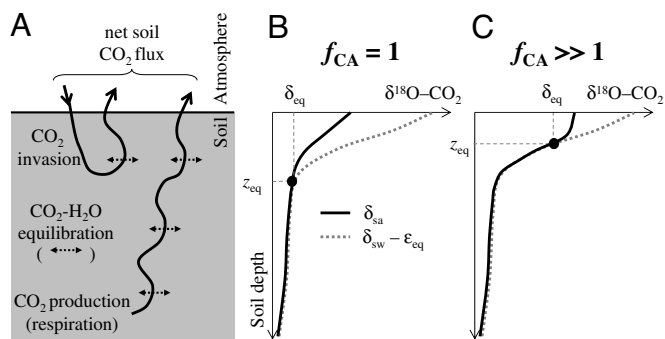


Fig. 1. Schematic showing the influence of CO₂ hydration rates on vertical profiles of $\delta^{18}\text{O}$ in soil air CO₂. (A) The net soil-atmosphere CO₂ exchange is composed of CO₂ molecules moving from the atmosphere into the soil and back to the atmosphere (i.e., invasion) and further CO₂ molecules produced during soil respiration. Because of oxygen isotopic exchange between soil CO₂ and water, both invasion and respiration fluxes modify the isotopic composition of atmospheric CO₂, and their ^{18}O isotopic signature depend on the extent of CA activity in the soil. (B) Typical profile of $\delta^{18}\text{O}$ in soil air CO₂ (δ_{sa}) for uncatalyzed CO₂ hydration in soil water (enhancement factor $f_{\text{CA}} = 1$). (C) Same as in B but for catalyzed CO₂ hydration (enhancement factor $f_{\text{CA}} \gg 1$). In deep soil layers where vertical gradients of δ_{sw} are weak, the residence time of CO₂ is long enough to reach full isotopic equilibrium with soil water ($\delta_{\text{sa}} = \delta_{\text{sw}} - \epsilon_{\text{eq}}$), where ϵ_{eq} denotes the isotopic equilibrium fractionation between CO₂ and water (22). Above a certain depth z_{eq} (where, by definition, $\delta_{\text{sa}} = \delta_{\text{eq}}$), CO₂ molecules diffuse too rapidly to fully equilibrate with local soil water. If CO₂ hydration is enhanced because of CA activity ($f_{\text{CA}} \gg 1$), the equilibration becomes faster and z_{eq} shallower, thus δ_{eq} becomes more enriched.

because the abundance and location of CA in soils is still somewhat unclear, with only indirect and isolated indications based on measurements of $\delta^{18}\text{O}$ of soil CO₂ or COS fluxes (14, 16, 17). Substantial CA activity in soils would lead to a faster equilibration of CO₂, moving z_{eq} further toward the surface where soil water is more ^{18}O enriched (Fig. 1 B and C). So far global simulations have assumed uncatalyzed CO₂ hydration in soils (18–20) and equilibration depths below the region of strong evaporative enrichment (5, 21).

Results and Discussion

Evidence for Enhanced Soil CO₂ Hydration Rates. Here, we demonstrate that, in contrast to current assumptions, the observed rate of soil CO₂ hydration is always substantially faster than the uncatalyzed rate. We compared measurements of depth-resolved soil water $\delta^{18}\text{O}$ (δ_{sw}) and observed $\delta^{18}\text{O}$ signatures of chamber-based soil CO₂ fluxes (δ_{flux}) in seven different ecosystems that encompass most of the major land biomes, providing a global perspective of ^{18}O exchange in soils (Table S1 and see Tables S5–S7). From the δ_{sw} data, we determined the depth-resolved $\delta^{18}\text{O}$ of soil CO₂ in full equilibrium with soil water (δ_{eq}), equal to $\delta_{\text{sw}} - \epsilon_{\text{eq}}$ where ϵ_{eq} is the temperature-sensitive equilibrium fractionation between CO₂ and water (22). Most sites exhibited strong gradients in $\delta_{\text{sw}} - \epsilon_{\text{eq}}$ at the soil surface, reflecting the evaporative enrichment of soil water (Fig. 2). From the δ_{flux} data, we determined the $\delta^{18}\text{O}$ of soil CO₂ at z_{eq} (δ_{eq} , see Fig. 1) for different rates of hydration expressed as an enhancement factor (f_{CA}) with respect to the uncatalyzed CO₂ hydration rate (see Eq. 6 in Methods). Increasing f_{CA} shifts z_{eq} toward surface layers (Fig. 2) and δ_{eq} toward δ_{a} . The best estimate for f_{CA} would be one in agreement with both soil water and chamber flux measurements. This is obtained when the point ($\delta_{\text{eq}}, z_{\text{eq}}$) derived from the chamber data intersects the δ_{eq} curve derived from soil water measurements. At all sites, this intersection occurs for values of f_{CA} between 10 and 300, with the lowest f_{CA} in the cooler temperate ecosystems while higher f_{CA} were found at the Mediterranean and subtropical sites (Fig. 2). As a consequence, the equilibration depth z_{eq} was in most cases within the top 5 cm of the soil, the zone containing the strongest δ_{sw} gradients. A reduction in the effective diffusivity of soil CO₂ would also lead to shallower equilibration depths z_{eq} by increasing the residence time of CO₂ in soils, but it would not yield simultaneous solutions for both soil water and CO₂ flux isotope data (14). Thus, an enhanced CO₂ hydration rate is the only plausible mechanism to explain these chamber-based measurements.

Consistency with CA Activities in Soil Microorganisms. The uppermost soil layers host many bacterial, algal, and fungal species that produce intracellular and sometimes extracellular CAs (23–25). Based on a literature survey, we claim that this mixed population

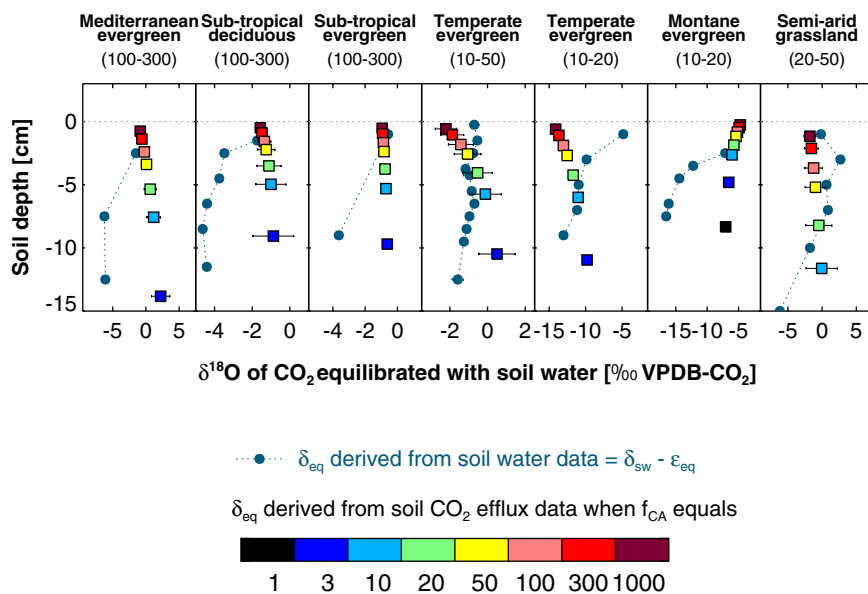


Fig. 2. The $\delta^{18}\text{O}$ of soil CO₂ at the depth of full equilibration ($\delta_{\text{eq}}, z_{\text{eq}}$; see Fig. 1) estimated from chamber flux measurements for different levels of hydration rates (f_{CA}). Depth-resolved soil water data yields the $\delta^{18}\text{O}$ of CO₂ in isotopic equilibrium with soil water ($\delta_{\text{sw}} - \epsilon_{\text{eq}}$). The point at which the two curves intersect indicates the most likely value for the enhancement factor, f_{CA} , listed below the ecosystem type for each site (see Table S1). The horizontal error bars on the squared symbols represent the standard deviation of δ_{eq} values over the number of δ_{flux} measurements ($n = 1$ –15).

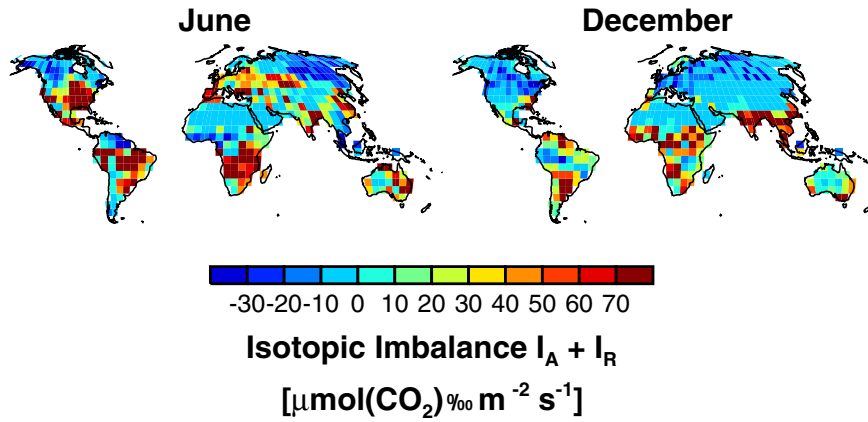


Fig. 4. Global distribution in the extent of isotopic imbalance ($I_A + I_R$) across continental surfaces for June and December simulated by the global model Mecbeth for the most enhanced soil CO_2 hydration scenario ($f_{CA} = 300$). Regions where $I_A + I_R$ is the most different from zero correspond to regions of strong isotopic imbalance where biospheric gross CO_2 fluxes are expected to be the most constrained by $\delta^{18}\text{O}$ data.

Future Directions for Global Isotope-Enabled Models. This study demonstrates that enhanced rates of CO_2 hydration occur at the soil surface and appreciably impact the oxygen isotope composition of atmospheric CO_2 . This enhanced exchange in the soil brings into focus our limited ability to predict the isotopic enrichment of soil water near the surface (18, 29), highlighting a need for future improvements in this research area. Also, although we provided the basic observations and parameterization, more work is now needed to further assess the variability in f_{CA} in different ecosystems, plant functional types, or regions within the global model, including attempts to establish the mechanistic basis to underpin the observed differences in CA activity between ecosystems. Developments on these fronts will greatly enhance our capabilities to use the $\delta^{18}\text{O}$ of atmospheric CO_2 to quantitatively inform us of large-scale changes in the intensity of carbon and water cycling in terrestrial ecosystems.

Methods

Soil CO^{18}O Budget Equation. In a given soil layer, the number of moles of CO^{18}O changes as a result of (i) CO^{18}O production during heterotrophic and autotrophic respiration, (ii) diffusion of these molecules through the soil layer, and (iii) oxygen isotopic exchange with the surrounding soil water (30–32):

$$\theta_t \frac{\partial C\mathcal{R}}{\partial t} = \mathcal{R}_c S_c + \frac{\partial}{\partial z} \left[D_{c,\text{iso}} \frac{\partial C\mathcal{R}}{\partial z} \right] + k_{h,\text{iso}} B \theta_w C (\mathcal{R}_{\text{eq}} - \mathcal{R}), \quad [1]$$

where C [$\text{mol}\cdot\text{mol}^{-1}$] is the CO_2 mole fraction in soil air, \mathcal{R} , \mathcal{R}_c , and \mathcal{R}_{eq} are the $^{18}\text{O}/^{16}\text{O}$ ratios of the CO_2 in soil air, respired CO_2 , and CO_2 in isotopic equilibrium with the surrounding soil water, respectively, S_c ($\text{mol}\cdot\text{m}^{-3}\cdot\text{s}^{-1}$) is the respiration rate density, $D_{c,\text{iso}}$ ($\text{m}^2\cdot\text{s}^{-1}$) is the effective diffusivity of CO^{18}O in soil air, θ_w ($\text{m}^3\cdot\text{m}^{-3}$) is the volumetric soil water content, B is the CO_2 solubility coefficient, and θ_t ($\text{m}^3\cdot\text{m}^{-3}$) is the total CO_2 porosity. Denoting by θ_a the soil air porosity we have (31): $\theta_t = \theta_a + B\theta_w$. The solubility coefficient B depends on soil temperature T_s (K) according to ref. 33: $B = 1.739\exp(-0.039(T_s - 273.15) + 0.000236(T_s - 273.15)^2)$. \mathcal{R}_{eq} is related to the $^{18}\text{O}/^{16}\text{O}$ ratio in soil water \mathcal{R}_{sw} through $\mathcal{R}_{\text{eq}} = (1 + \varepsilon_{\text{eq}})\mathcal{R}_{\text{sw}}$, where $\varepsilon_{\text{eq}} = 17.604/T_s - 0.01793$ is the CO_2 - H_2O equilibrium fractionation (22). Because there are three oxygen atoms present in the bicarbonate intermediate, the isotopic exchange rate during CO_2 hydration equals one-third the hydration rate (7): $k_{h,\text{iso}} = f_{CA}k_{h,\text{uncat}}/3$, where (34) $k_{h,\text{uncat}} = 0.037 \times \exp(0.118(T_s - 298.15))$. In this framework, CA activity is expressed as an enhancement factor (f_{CA}) of the uncatalyzed CO_2 hydration rate ($k_{h,\text{uncat}}$). The effective CO^{18}O diffusivity in soil air is calculated as $D_{c,\text{iso}} = D_{c,\text{eff}} \alpha_d$, where $\alpha_d = 0.9913$ is the isotopic discrimination during molecular diffusion of CO_2 in air and $D_{c,\text{eff}}$ ($\text{m}^2\cdot\text{s}^{-1}$) is the effective CO_2 diffusivity in soil air. Several parameterizations of this effective diffusivity exist in the literature that differ mostly for wet soils (35). Results presented in this study use ref. 31: $D_{c,\text{eff}} = 0.66 \times \theta_a \times 1.4 \cdot 10^{-5} (T_s/298.15)^{1.75}$.

Full Equilibration Depth. The budget equation above contains two time scales. One time scale indicates the half-life of CO_2 molecules before being isotopically equilibrated with the surrounding water:

$$\tau_k = \ln 2 \cdot \left(\frac{\theta_t}{k_{h,\text{iso}} B \theta_w} \right) \quad [2]$$

and another time scale indicates the time required for a plume of C^{18}O molecules to diffuse through the soil over a given distance z :

$$\tau_d(z) = \frac{\theta_t z^2}{2D_{c,\text{iso}}} \quad [3]$$

Full equilibration within a soil layer of thickness z is satisfied when the time scale for isotopic equilibration is smaller than the time scale for diffusion through this layer, i.e., $\tau_k \ll \tau_d(z)$. When $\tau_k = \tau_d(z)$, full equilibration can occur if the soil layer has uniform soil temperature, moisture content, and isotopic composition. However, in the top centimeters of the soil, strong gradients of T_s , θ_w , and \mathcal{R}_w are more likely. The shallowest depth of full equilibration, z_{eq} , must therefore satisfy the inequality: $\tau_k < \tau_d(z_{\text{eq}})$. In the following we will define z_{eq} as: $\tau_k = \tau_d(z_{\text{eq}})/4$, or similarly:

$$z_{\text{eq}} = 2 \sqrt{\frac{2 \ln 2 D_{c,\text{iso}}}{k_{h,\text{iso}} B \theta_w}} \quad [4]$$

The factor 4 was determined by matching the value of f_{CA} deduced in Fig. 2 with that obtained from simulations using the full numerical model (Eq. 1), i.e., $f_{CA} \approx 300$ for the Mediterranean evergreen site (14) and $f_{CA} \approx 20$ for the montane evergreen site (15). Eq. 4 with $f_{CA} = 20$ also provides seasonal variations of z_{eq} at the temperate evergreen site that correspond to the depth where $\delta^{18}\text{O}$ in soil air CO_2 (δ_{sa}) and $\delta_{\text{sw}} - \varepsilon_{\text{eq}}$ (estimated using the full numerical model, Eq. 1) start to diverge by >0.3 ‰ (a threshold chosen for practical purposes to represent the overall precision of soil water isotope measurements).

Other studies (14, 35) use a different formulation for $D_{c,\text{iso}}$, leading to values of this diffusivity 5-fold smaller in saturated soils. Using this other formulation does not fundamentally change the results presented in Fig. 2.

Soil CO_2 Isoflux. In the steady state, and assuming isothermal and uniform soil water conditions, Eq. 1 can also be solved analytically (30–32). In this framework, the isotopic composition of the soil CO_2 flux δ_{flux} is:

$$\delta_{\text{flux}} = \delta_{\text{eq}} + \varepsilon_{d,\text{eff}} + (\delta_{\text{eq}} - \delta_a) v_{\text{inv}} \frac{C_a}{F_R}, \quad [5]$$

where $\varepsilon_{d,\text{eff}}$ is the effective isotopic fractionation during diffusion, F_R is the soil CO_2 efflux, and $v_{\text{inv}} = \sqrt{B\theta_w k_{h,\text{iso}} D_{c,\text{iso}}}$ has the dimensions of a velocity ($\text{m}\cdot\text{s}^{-1}$) that when multiplied by C_a gives the soil invasion flux F_{inv} . The product $(\delta_{\text{flux}} - \delta_a)F_R$ is called the soil CO_2 isoflux. It can be seen as the sum of two isotope fluxes: a respiration isoflux, $I_R = (\delta_{\text{eq}} + \varepsilon_{d,\text{eff}} - \delta_a)F_R$, and an invasion isoflux, $I_{\text{inv}} = (\delta_{\text{eq}} - \delta_a)F_{\text{inv}}$, sometimes defined as abiotic because it is independent of

F_R . Assuming a uniform soil CO_2 production S_c over a soil column of depth z_0 , $\varepsilon_{d,\text{eff}}$ can be estimated as (31): $\varepsilon_{d,\text{eff}} = \varepsilon_d(1 - z_1/z_0(1 - \exp(-z_0/z_1)))$, where $z_1 = (2\sqrt{2\ln 2})^{-1} z_{\text{eq}}$. Eq. 5 can then be inverted to estimate δ_{eq} as a function of δ_{flux} , C_a , δ_a , and F_R measurements:

$$\delta_{\text{eq}} = \frac{\delta_{\text{flux}} - \varepsilon_{d,\text{eff}} + v_{\text{inv}}C_a/F_R\delta_a}{1 + v_{\text{inv}}C_a/F_R} \quad [6]$$

Oxygen Isotope Composition of the Net CO_2 Flux from Soil Chambers. The steady-state oxygen isotope signal of the net soil CO_2 flux during chamber closure (δ_{ch}) was calculated by using a simple isotopic mass balance:

$$\delta_{\text{ch}} = \frac{\delta_{\text{out}}C_{\text{out}} - \delta_{\text{in}}C_{\text{in}}}{C_{\text{out}} - C_{\text{in}}}, \quad [7]$$

where C_{out} , C_{in} and δ_{out} , δ_{in} are the mole fractions and isotopic compositions of CO_2 in the air leaving and entering the chamber, respectively. In the case of the two sites that used closed chambers (subtropical evergreen and semiarid grassland), C_{out} , C_{in} and δ_{out} , δ_{in} are the mole fractions and isotopic compositions of CO_2 at the start and end of a defined chamber closure period, respectively.

To derive δ_{eq} values from soil chamber data, we use Eq. 6, neglect chamber effects, and make the common assumption that the atmosphere inside the chamber is well mixed ($C_a = C_{\text{out}}$ and $\delta_a = \delta_{\text{out}}$).

Oxygen Isotope Composition of Soil Water. Depth-resolved soil samples were collected at each experimental site within proximity of the soil chamber and at approximately the same time as gas exchange measurements. In the case of the Mediterranean evergreen, subtropical evergreen, and both temperate ever-

green sites, soil water was extracted cryogenically from bulk soil samples and $\delta^{18}\text{O}$ analysis of CO_2 equilibrated with the extracted water was completed (14). For the montane evergreen, subtropical deciduous, and semiarid grassland sites CO_2 with a known isotopic composition was equilibrated directly with fresh soil samples and stored in gas-tight containers for 12 h. Equilibrated CO_2 was then sampled from the container and analyzed for its $\delta^{18}\text{O}$ composition (15).

Global Model Simulations. The global model Mecbeth calculates the sources and sinks of CO_2 , water, and their respective isotopes and transports them in the atmosphere (18, 19). It merges a description of the biospheric energy, water, and carbon fluxes with a global climate and water isotope model. The atmosphere and biosphere are dynamically coupled to account for feedbacks of the accelerated equilibration of CO_2 with soil water on δ_a and the isotopic signatures of leaf and other fluxes. The model parameterization of soil water isotopes was improved in this study to provide depth-resolved descriptions of soil water and soil water isotopes (35), a necessary step if CA activity occurs in soils containing strong vertical gradients in δ_{sw} (14). Several soil layers of varying thickness were included in the model. The most important upper layers relevant to this study consisted of a top layer at 0–6 cm and another layer at 6–20 cm.

ACKNOWLEDGMENTS. We thank P. Richard for isotopic analysis of the soil water data from Le Bray, France and W. T. Baisden for contributions to the sample collection at Canterbury, New Zealand. L.W. was supported by the CarboEurope-IP research program funded by the European Union. Soil CA assays were made possible through funding from the Institut National de la Recherche Agronomique Projet Innovant, Centre National de la Recherche Scientifique Ecosystèmes Continentaux et Risques Environnementaux and Région Provence-Alpes-Côte d'Azur.

- Intergovernmental Panel on Climate Change (2007) *Climate Change 2007—The Physical Sciences Basis: Contribution of Working Group I to the Fourth Assessment Report of the Intergovernmental Panel on Climate Change* (Cambridge Univ Press, Cambridge, UK).
- Davidson EA, Janssens IA (2006) Temperature sensitivity of soil carbon decomposition and feedbacks to climate change. *Nature* 440:165–173.
- Friedlingstein P, et al. (2006) Climate-carbon cycle feedback analysis: Results from the C⁴MIP model intercomparison. *J Clim* 19:3337–3353.
- Francey RJ, Tans PP (1987) Latitudinal variation in oxygen-18 of atmospheric CO_2 . *Nature* 327:495–497.
- Farquhar GD, et al. (1993) Vegetation effects on the isotope composition of oxygen in atmospheric CO_2 . *Nature* 363:439–443.
- Yakir D, Wang X-F (1996) Fluxes of CO_2 and water between terrestrial vegetation and the atmosphere estimated from isotope measurements. *Nature* 380:515–517.
- Mills GA, Urey HC (1940) The kinetics of isotopic exchange between carbon dioxide, bicarbonate ion, carbonate ion and water. *J Am Chem Soc* 62:1019–1026.
- Silverman DN (1982) Carbonic anhydrase: Oxygen-18 exchange catalyzed by an enzyme with rate-contributing proton-transfer steps. *Methods Enzymol* 87:732–752.
- Gillon JS, Yakir D (2001) Influence of carbonic anhydrase activity in terrestrial vegetation on the ^{18}O content of atmospheric CO_2 . *Science* 291:2584–2587.
- Dongmann G, Nürnberg HW, Förstel H, Wagener K (1974) On the enrichment of H_2^{18}O in the leaves of transpiring plants. *Radiat Environ Biophys* 11:41–52.
- Farquhar GD, Cernusak LA, Barnes B (2007) Heavy water fractionation during transpiration. *Plant Physiol* 143:11–18.
- Ogée J, et al. (2004) Partitioning net ecosystem carbon exchange into net assimilation and respiration with canopy-scale isotopic measurements: An error propagation analysis with $^{13}\text{CO}_2$ and CO^{18}O data. *Global Biogeochem Cycles*, 2010.1029/2003GB002166.
- Barnes CJ, Allison GB (1988) The distribution of deuterium and oxygen-18 in dry soils: I. Theory. *J Hydrol* 60:141–156.
- Wingate L, et al. (2008) Oxygen stable isotope signals of net soil CO_2 efflux record changes in soil evaporation and indicate the presence of carbonic anhydrase in Mediterranean soils. *Global Change Biol* 14:2178–2193.
- Miller JB, Yakir D, White JMC, Tans PP (1999) Measurements of $^{18}\text{O}/^{16}\text{O}$ in the soil-atmosphere CO_2 flux. *Global Biogeochem Cycles* 13:761–774.
- Seibt U, Wingate L, Lloyd J, Berry J (2006) Diurnally variable $\delta^{18}\text{O}$ signatures of soil CO_2 fluxes indicate carbonic anhydrase activity in a forest soil. *J Geophys Res*, 10.1029/2006JG000177.
- Kesselmeier J, Teusch N, Kuhn U (1999) Controlling variables for the uptake of atmospheric carbonyl sulfide by soil. *J Geophys Res* 104:11577–11584.
- Cuntz M, et al. (2003) A comprehensive global three-dimensional model of $\delta^{18}\text{O}$ in atmospheric CO_2 : 2. Mapping the atmospheric signal. *J Geophys Res*, 4510.1029/2002JD003154:002003.
- Cuntz M, Ciais P, Hoffmann G, Knorr W (2003) A comprehensive global three-dimensional model of $\delta^{18}\text{O}$ in atmospheric CO_2 : 1. Validation of surface processes. *J Geophys Res*, 4510.1029/2002JD003153.
- Stern L, Amundson R, Baisden WT (2001) Influence of soils on oxygen isotope ratio of atmospheric CO_2 . *Global Biogeochem Cycles* 15:753–759.
- Peylin P, et al. (1999) A 3-dimensional study of $\delta^{18}\text{O}$ in atmospheric CO_2 : Contribution of different land ecosystems. *Tellus* 51B:642–667.
- Brenninkmeijer CAM, Kraft P, Mook WG (1983) Oxygen isotope fractionation between CO_2 and water. *Isotope Geosci* 1:181–190.
- Smith KS, Ferry JG (2000) Prokaryotic carbonic anhydrases. *FEMS Microbiol Rev* 24:335–366.
- Badger MR, Price GD (1994) The role of carbonic anhydrase in photosynthesis. *Annu Rev Plant Physiol Plant Mol Biol* 45:369–392.
- Moroney JV, Bartlett SG, Samuelsson G (2000) Carbonic anhydrases in plants and algae. *Plant Cell Environ* 24:141–153.
- Trolier M, White JWC, Tans PP, Masarie KA, Gemery PA (1996) Monitoring the isotopic composition of atmospheric CO_2 : Measurements from the NOAA global air sampling network. *J Geophys Res* 101:25897–25916.
- Allison CE, Francey RJ (2007) Verifying Southern Hemisphere trends in atmospheric carbon dioxide stable isotopes. *J Geophys Res*, 21310.21029/22006JD00734.
- Ciais P, et al. (1997) A three-dimensional synthesis study of $\delta^{18}\text{O}$ in atmospheric CO_2 . 1. Surface fluxes. *J Geophys Res* 102:5857–5872.
- Cornwell AR, Harvey LDD (2007) Soil moisture: A residual problem underlying AGCMs. *Clim Change* 84:313–336.
- Hesterberg R, Siegenthaler U (1991) Production and stable isotopic composition of CO_2 in a soil near Bern, Switzerland. *Tellus* 43:197–205.
- Tans PP (1998) Oxygen isotopic equilibrium between carbon dioxide and water in soils. *Tellus* 50:163–178.
- Amundson R, Stern L, Baisden WT, Wang Y (1998) The isotopic composition of soil and soil-respired CO_2 . *Geoderma* 82:83–114.
- Weiss RF (1974) Carbon dioxide in water and seawater: The solubility of nonideal gas. *Mar Chem* 2:203–215.
- Skirrow G (1975) The dissolved gases: Carbon dioxide. *Chemical Oceanography*, eds Riley JP, Skirrow G (Academic, San Diego), Vol 2, pp 1–92.
- Riley WJ, Still CJ, Torn MS, Berry JA (2002) A mechanistic model of H_2^{18}O and CO^{18}O fluxes between ecosystems and the atmosphere: Model description and sensitivity analysis. *Global Biogeochem Cycles*, 1010.1029/2002GB001878.